

Exotic Superconductivity Through Bosons in a Dynamical Cluster Approximation

Thomas Bilitewski*

T.C.M. Group, Cavendish Laboratory, J.J. Thomson Avenue, Cambridge CB3 0HE, United Kingdom

Lode Pollet

Department of Physics, Arnold Sommerfeld Center for Theoretical Physics, and Center for Nanoscience, Ludwig-Maximilians-Universität München, Theresienstraße 37, 80333 Munich, Germany

(Dated: August 14, 2018)

We study the instabilities towards (exotic) superconductivity of mixtures of spin-1/2 fermions coupled to scalar bosons on a two-dimensional square lattice with the Dynamical-Cluster-Approximation (DCA) using a numerically exact continuous-time Monte-Carlo solver. The Bogoliubov bosons provide an effective phononic bath for the fermions and induce a non-local retarded interaction between the fermions, which can lead to (exotic) superconductivity. Because of the sign problem the biggest clusters we can study are limited to 2×2 in size, but this nevertheless allows us to study the pairing instabilities, and their possible divergence, in the s - and d -wave channels as well as the competition with antiferromagnetic fluctuations. At fermionic half-filling we find that d -wave is stable when the mediated interaction by the bosons is of the same order as the bare fermionic repulsion. Its critical temperature can be made as high as the maximum one for s -wave, which opens perspectives for its detection in a cold atom experiment.

I. INTRODUCTION

Mixtures of bosons and fermions are ubiquitous: They are fundamental in particle physics, where bosons are the carriers of forces between fermionic matter particles. In condensed matter systems, they appear in the context of superconductivity, where the conventional pairing mechanism consists of phonons inducing an effective retarded attractive interaction between electrons leading to the formation of Cooper-pairs, as well as in mixtures of ^3He and ^4He in which the inter- and intra-isotope interactions are of comparable magnitude. Cold-atom systems are uniquely suited to simulate this physics as they allow fine experimental control over the interactions as well as the tunnelling amplitudes^{1,2}.

The optical lattice system does not have phonons. Nevertheless, pairing mechanisms with cold fermions in an optical lattice can be investigated by quantum simulation. Bosons deep in the superfluid phase have a linear dispersion³ which can play the role of phonons as in conventional superconductors (when fermions form an electron gas) but, as we will see, they can equally well couple to spin density wave fluctuations (relevant when the charge of the fermions is near localization). Spin density wave fluctuations induce an attractive interaction between electrons in a spin-singlet, with the pair wavefunction changing sign between different regions of the Fermi surface⁴⁻¹³. It plays a prominent role in the cuprates (where it correctly predicts d -wave pairing), the iron superconductors and heavy fermion materials¹⁴⁻²³. The fermionic Hubbard repulsion and the lattice dispersion can, in principle, be changed in a cold-atom experiment and allow to systematically investigate the interplay of both pairing mechanisms.

Quantum degenerate mixtures of bosonic and spin-polarized fermionic species have first been realized experimentally with ^{23}Na and ^6Li ²⁴. Since then a variety of different species combinations have been employed

in experiments and these systems have been studied extensively²⁵⁻⁴⁵. Recently, using ^6Li and ^7Li a system has been realised experimentally for the first time in which both bosonic and spinful fermionic species are superfluid⁴⁶, giving rise to induced interactions in the bosonic sector due to excitations of the fermionic superfluid^{47,48}. Another promising candidate for experiments with spinful mixtures are ^{23}Na and ^{40}K in which a large number of interspecies Feshbach resonances at experimentally accessible magnetic fields have been identified enabling the tuning of the interspecies interactions and the simulation of boson-induced interactions between the fermions^{49,50} and the creation of stable fermionic Feshbach molecules⁵¹.

Theoretically, the interactions mediated by superfluid bosons⁵² were studied in the regime where the sound velocity of the bosons is fast compared to the Fermi velocity and found to be attractive and capable of overcoming a sufficiently weak repulsive fermi interactions leading to s -wave pairing both in the continuum^{52-57,60-62} and in optical lattices^{3,58,59}. Recently, the phase diagram of Bose-Fermi mixtures in 3 dimensional optical lattices has been studied numerically within the DMFT-formalism⁶³ and analytically in a mean-field treatment⁶⁴ finding such phases as charge-density waves, superfluidity in either or both sectors, and supersolids. In 2 dimensional lattices the competition between s - and d -wave superfluidity and antiferromagnetic phases was investigated using the functional renormalization group⁶⁵.

In this work we restore some momentum fluctuations compared to the aforementioned DMFT study by studying mixtures in the Fermi liquid regime in a DCA framework in two dimensions and monitor the pairing susceptibilities. We assume that the bosons are deep in the superfluid phase which allows to find (exotic) pairing channels (unlike single-site DMFT) and the interplay with anti-ferromagnetic fluctuations but it

rules out charge density wave order. We find that the bosonic condensate can enhance both s - and d -wave pairing. Just as in conventional superconductors s -wave pairing is possible for weakly repulsive bare fermions. However, as the lattice effects and the bare Hubbard repulsion grow in importance, d -wave takes over and can be the dominant pairing channel. Atomic Bose-Fermi mixtures thus effectively display two different pairing mechanisms, relevant for superconductors.

II. MODEL

Our system is described by the fermionic action $S = S_f + S_{\text{ret}}$, with

$$S_f = \int_0^\beta d\tau \sum_{\langle i,j \rangle, \sigma} \bar{c}_i^\sigma(\tau) [\delta_{i,j} (\partial_\tau - \mu_f + n_0 U_{\text{bf}}) - t_f] c_j^\sigma(\tau) + U_{\text{ff}} \sum_i n_{i,\uparrow}^f(\tau) n_{i,\downarrow}^f(\tau) \quad (1)$$

$$S_{\text{ret}} = -\frac{n_0 U_{\text{bf}}^2}{2} \iint_0^\beta d\tau_1 d\tau_2 \sum_{i,j} n_i^f(\tau_1) D_{ij}(\tau_1 - \tau_2) n_j^f(\tau_2).$$

It describes a fermionic Hubbard model with hopping amplitude t_f , on-site repulsion U_{ff} and chemical potential μ_f coupled to bosons deep in the condensed phase with condensate density n_0 via an on-site density-density coupling U_{bf} . The bosons are treated in the Bogoliubov approximation and subsequently integrated out, giving rise to the chemical potential shift $n_0 U_{\text{bf}}$ and the non-local retarded density-density action term S_{ret} with kernel

$$D(i-j, \tau) = \iint_{B.Z.} \frac{d^2 k}{(2\pi)^d} e^{i\mathbf{k}(\mathbf{r}_i - \mathbf{r}_j)} \frac{e^{E_{\mathbf{k}}\tau} + e^{E_{\mathbf{k}}(\beta - \tau)}}{e^{\beta E_{\mathbf{k}}} - 1} \frac{|\bar{\varepsilon}_{\mathbf{k}}|}{E_{\mathbf{k}}} \quad (2)$$

where $E_{\mathbf{k}} = [\bar{\varepsilon}_{\mathbf{k}}^2 + 2\bar{\varepsilon}_{\mathbf{k}} n_0 U_{\text{bb}}]^{1/2}$ is the dispersion of the Bogoliubov quasi-particles, $\bar{\varepsilon}_{\mathbf{k}} = \varepsilon_{\mathbf{k}} - \varepsilon_0$ the lattice dispersion of the bare bosons, shifted to be positive, and U_{bb} the repulsion between the bare bosons on the lattice. The chemical potential μ_b was fixed to give unit filling for the bosons (its density is unimportant in the superfluid regime). The explicit construction from the underlying Hamiltonian is performed in Appendix A. This treatment neglects any back-action of the fermions on the bosons, in particular, bosonic charge order is excluded, which might be mediated from the fermionic sector by the density-density coupling between bosons and fermions. However, for fast bosons (amounting to $t_b > t_f$) which we consider, charge-density ordering was found to be suppressed and superconductivity to be favored in DMFT⁶³.

In the instantaneous limit, *i.e.*, the case of a very high bosonic speed of sound compared to the Fermi velocity as it can be made in the NaK system³, this simplifies to $D_{\text{inst}}(\mathbf{k}) = \frac{1}{n_0 U_{\text{bb}}} c(\mathbf{k}) =$

$\frac{1}{n_0 U_{\text{bb}}} \{1 + \xi^2 [4 - \cos(k_x) - \cos(k_y)]\}^{-1}$, with $\xi = \sqrt{t_b / (2U_{\text{bb}})}$ as obtained in⁶⁵. The induced on-site interaction is given by $W = \frac{U_{\text{bf}}^2}{U_{\text{bb}}} \sum_{\mathbf{k}} c(\mathbf{k})$, thus scaling as $V = U_{\text{bf}}^2 / U_{\text{bb}}$. The bosonic dispersion $E_{\mathbf{k}}$ can only have an influence on the fermionic system if ξ is comparable to the lattice spacing, which is satisfied for NaK.

III. METHODOLOGY

To numerically study the action Eq. (1) we use the dynamical cluster approximation (DCA)^{66–68}, which maps the many-body problem onto a self-consistently embedded cluster impurity problem. Its action $S = S_0 + S_{\text{int}}$ reads

$$S_0 = \int_0^\beta d\tau \sum_{i,j,\sigma} \bar{c}_i^\sigma(\tau_1) \mathcal{G}_{\sigma,i,j}^{-1}(\tau_1 - \tau_2) c_j^\sigma(\tau_2) \quad (3)$$

$$S_{\text{int}} = U_{\text{ff}} \sum_i n_{i,\uparrow}^f(\tau) n_{i,\downarrow}^f(\tau) + S_{\text{ret}} \quad (4)$$

Here, the sums run over the cluster degrees of freedom, \mathcal{G} is the unknown cluster-excluded Green's function of the impurity problem which has to be determined self-consistently. The local Hubbard interaction U_{ff} remains unaffected by the DCA mapping, but the non-local induced interaction is coarse-grained, *i.e.*, D_{ij} in S_{ret} is replaced by \bar{D}_{ij} , which is the Cluster-Fourier transform of the coarse-grained interaction kernel $D(i-j)$.

To solve the impurity problem, we use a generalized weak-coupling solver^{69,70} to include the non-local phononic degrees of freedom similar as in Ref.⁷¹. We are limited to 2×2 clusters because of the sign problem, which also occurs at half filling because the induced interactions, $\bar{D}_{i,j}(\tau)$ (Eq. 2), do not have a definite sign. Results of the average sign for characteristic values of the parameters and temperatures used in our simulations are shown in Appendix B. Unfortunately, 2×2 clusters are known to overestimate the d -wave transition temperature and to strongly suppress antiferromagnetic phases^{68,72}. Bigger clusters are highly desired to take the Kosterlitz-Thouless transitions properly into account, but are out of reach.

To obtain transitions to a superconducting state we need to consider the two-particle Green's function for opposite spin pairing in the particle-particle channel

$$\chi(q, k, k') = \int_0^\beta \int_0^\beta \int_0^\beta \int_0^\beta d\tau_1 d\tau_2 d\tau_3 d\tau_4 \times e^{i[(\omega_n + \nu)\tau_1 - \omega_n \tau_2 + \omega_{n'} \tau_3 - (\omega_{n'} + \nu)\tau_4]} \langle T_\tau P(\cdot) \rangle \quad (5)$$

$$P(\cdot) = c_{\mathbf{k}+\mathbf{q},\sigma}^\dagger(\tau_1) c_{-\mathbf{k},-\sigma}^\dagger(\tau_2) c_{-\mathbf{k}',-\sigma}(\tau_3) c_{\mathbf{k}'+\mathbf{q},\sigma}(\tau_4)$$

where we adopt the notation $k = (\mathbf{k}, i\omega_n)$, $k' = (\mathbf{k}', i\omega_{n'})$ and $q = (\mathbf{q}, i\nu_n)$ ⁷³. For transitions to states of lower symmetry than the lattice, the Green's function

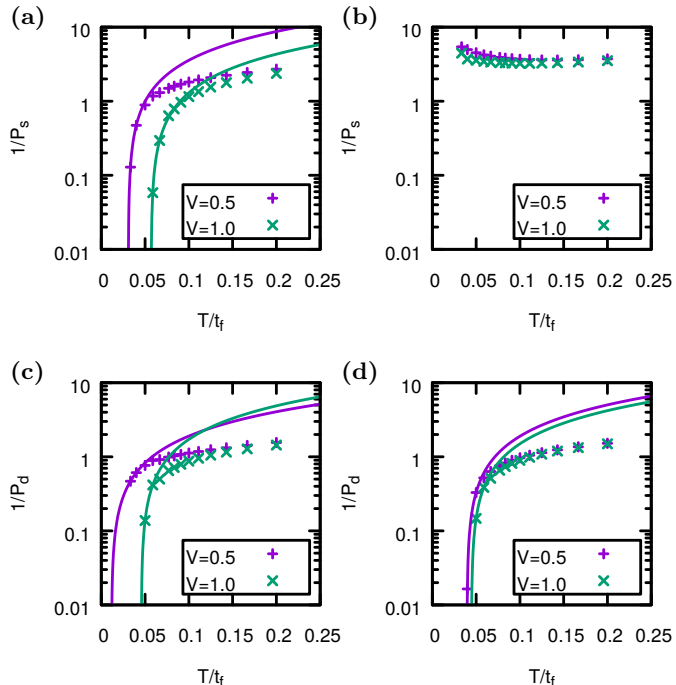


Figure 1. Inverse pairing field susceptibility $1/P_g$ on a logarithmic scale for $g = s(d)$ -wave symmetry at the top (bottom) at fixed $U_{\text{ff}} = 0(1)$ at the left (right) and fermionic half filling as a function of temperature for different coupling strength U_{bf} to the bosons corresponding to $V = 0.5, 1.0$ for the bosonic parameters $U_{\text{bb}}/t_{\text{f}} = 5$ and $t_{\text{b}}/t_{\text{f}} = 10$. The vanishing of $1/P_g$ signals the transition to a superconducting state of the corresponding symmetry. The solid lines are linear fits to the lowest temperature points and are used to derive T_c .

needs to be projected according to

$$\Pi_{g,g}(q, k, k') = g(\mathbf{k})\chi(q, k, k')g(\mathbf{k}') \quad (6)$$

where $g(\mathbf{k})$ is the form-factor for the corresponding symmetry. The pairing susceptibility is then given by

$$P_g(q, T) = \frac{T^2}{N_c^2} \sum_{K, K'} \bar{\Pi}_{g,g}(q, K, K'). \quad (7)$$

where $\bar{\Pi}$ is the coarse-grained version of $\Pi_{g,g}$ obtained by inverting the coarse-grained Bethe-Salpeter equation as described in⁶⁷. The calculation of the corresponding quantity for pairing in the particle-hole channel, relevant for transitions to an antiferromagnetic state, is similar and explained in detail in⁶⁸.

IV. RESULTS

We now turn to the investigation of the fermionic instabilities, which is reflected in the behavior of susceptibilities in the particle-hole and particle-particle

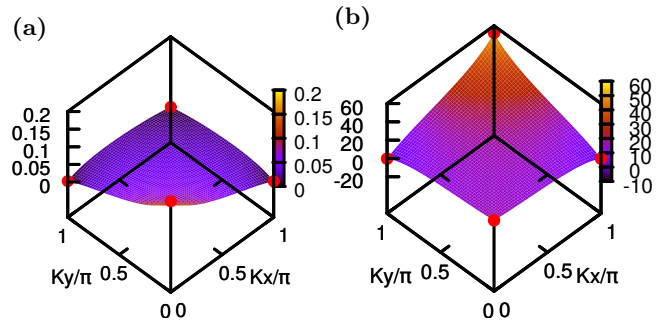


Figure 2. Pairing vertex in the particle-particle channel $\Gamma_{\text{PP}}^P(\mathbf{K} - \mathbf{K}')$ as a function of the relative momentum for $U_{\text{ff}}/t_{\text{f}} = 0.2$, $V/t_{\text{f}} = 2$ in (a) where s -wave pairing dominates showing a peak at $\mathbf{K} - \mathbf{K}' = (0, 0)$ and for $U_{\text{ff}}/t_{\text{f}} = 5$, $V/t_{\text{f}} = 1$ in (b) where d -wave pairing dominates displaying a clear peak at $\mathbf{K} - \mathbf{K}' = (\pi, \pi)$.

channels, specifically the antiferromagnetic susceptibility χ_{AF} at momentum transfer $q = ((\pi, \pi), 0)$ and the pairing field susceptibility P_g as defined in Eq. (7) for the dominant momentum transfer $q = (0, 0)$ in the case of the s -, extended s -, p - and d -wave symmetry^{67,72}. The divergence of the pairing field signals the phase transition to the state of the corresponding symmetry. To obtain the respective transition temperature we fit a linear function to the pairing fields in the low-temperature region as is appropriate for the mean-field nature of DCA close to T_c ^{68,72}. At half filling, we only found transitions to s - and d -wave, as well as strong antiferromagnetic correlations, whose competition is the focus of what follows.

The $s(d)$ -wave pairing fields with the linear fits are shown in the upper (lower) panel of Fig. (1). In the free model ($U_{\text{ff}} = U_{\text{bf}} = 0$) there is no pairing in either channel. When increasing U_{bf} (but keeping $U_{\text{ff}} = 0$), competing s - and d -wave instabilities develop as seen in the left panel. For $U_{\text{bf}}/t_{\text{f}} = 1.58$, *i.e.*, $V/t_{\text{f}} = 0.5$, we observe that the extrapolated s -wave transition temperature is higher than the d -wave one and s -wave pairing is thus the dominant channel. For weak V the mechanism for induced s -wave superconductivity is the same as in BCS theory. Upon increasing V , the s -wave gap becomes stronger and we enter the regime where superconductors are routinely described by the Migdal-Eliashberg theory^{60,74-79}. The momentum dependence of the bosonic dispersion E_k is here unimportant but retardation effects do matter in general. A selfconsistent treatment of the bosons (*e.g.*, via a damping term) is left for future work.

Upon increasing U_{ff} s -wave-pairing is suppressed and d -wave is the dominant instability as seen in the right panel for $U_{\text{ff}}/t_{\text{f}} = 1$ where no s -wave instability is found for the range of V shown. This is easily understood in the instantaneous limit where W scales with $V = U_{\text{bf}}^2/U_{\text{bb}}$ and for $|W| < |U_{\text{ff}}|$ no s -wave pairing is possible.

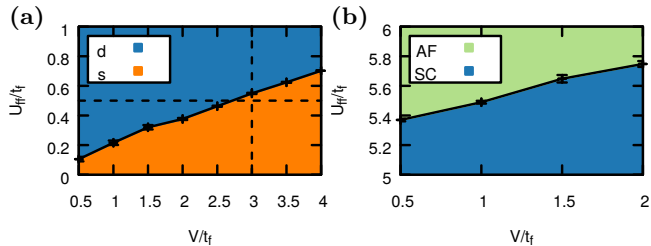


Figure 3. (a) Phase diagram based on the transition temperatures obtained from the linear extrapolation of the inverse pairing field susceptibilities P_g for the competing instabilities towards s - and d -wave pairing for bosonic parameters $U_{bb}/t_f = 5$ and $t_b/t_f = 10$. The phase transition line corresponds to the critical coupling U_{ff}^c where the computed transition temperatures for the respective phases cross. The dashed lines correspond to the cuts along which the transition temperatures are shown in Fig. 4. (b) Phase diagram focusing on the transition between the cluster antiferromagnetic instability ('AF') and the superconducting phase ('SC').

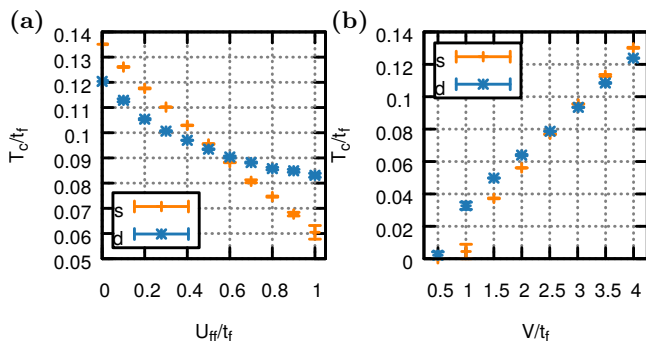


Figure 4. Critical temperature T_c for s - and d -wave pairing as a function of U_{ff} at fixed $V/t_f = 3$ in (a) and as a function of V at fixed $U_{ff}/t_f = 0.5$ in (b).

The competition between s - and d -wave pairing is also clearly reflected in the momentum structure of the pairing vertex shown in Fig. (2) in (a) for a situation where s -wave dominates and in (b) where d -wave is dominant. In the case of s -wave pairing the vertex peaks at a zero momentum transfer leading to a homogeneous real space structure whereas for d -wave a strong peak develops for a momentum transfer $\mathbf{K} - \mathbf{K}' = (\pi, \pi)$ leading to oscillatory behaviour in real space.

Based on the extrapolated transition temperatures we obtain the phase-diagram in Fig (3)(a). For the bosonic parameters $U_{bb}/t_f = 5$ and $t_b/t_f = 10$ we have that $W \approx 0.25V$ and we expect s -wave pairing to become relevant around $V \approx 4W \sim 4|U_{ff}|$. Indeed, on increasing U_{bf} we first observe increasing transition temperatures for d -wave pairing up to the regime $|W| \gtrsim |U_{ff}|$.

The critical temperatures for s - and d -wave pairing along cuts in the phase-diagram are shown in Fig (4). As the 2×2 cluster represents the mean-field result

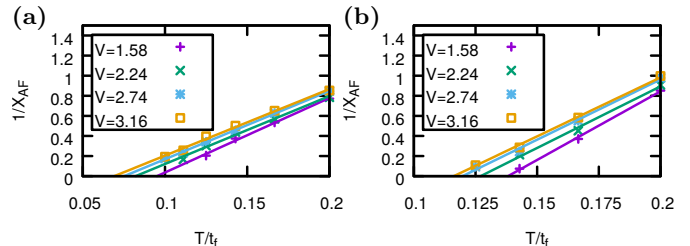


Figure 5. Inverse pairing field susceptibility $1/\chi_{AF}$ as a function of temperature T/t_f at fixed $U_{ff} = 5.2(5.8)$ to the left (right) and fermionic half filling for different coupling strength U_{bf} to the bosons corresponding to $V = 0.5, 1.0, 1.5, 2.0$ for the bosonic parameters $U_{bb}/t_f = 5$ and $t_b/t_f = 10$. The vanishing of $1/P_{AF}$ signals the transition to an AFM state. The solid lines are linear fits to the lowest temperature points and are used to derive T_c .

for d -wave, underestimating the fluctuations and consequently overestimating the d -wave transition temperatures, we expect the transition line to shift in favor of s -wave in those regions in which the s -wave transition temperature is finite, *i.e.*, qualitatively those for which the effective induced interaction W is stronger than the repulsion given by U_{ff} .

Next we consider the instability towards an antiferromagnetic state. In the thermodynamical limit antiferromagnetism is allowed at zero temperature only but in selfconsistent cluster approaches such as DCA it can be found at finite temperature as well, rather accurately reproducing correlations at short distances but missing their fluctuations at long distances.

The spin susceptibility $\chi_{AF}(T)$, corresponding to an instability in the spin sector of the particle-hole channel, is shown in Fig. 5 for $U_{ff} = 5.2, 5.8$ and for different values of the strength of the induced interaction $V = 0.5, 1.0, 1.5, 2.0$. To obtain the Neel temperature which corresponds to the divergence of $\chi_{AF}(T)$ a linear function to the inverse spin susceptibility in the low-temperature region is used as explained above.

Based on the extrapolated transition temperatures for the divergence of the antiferromagnetic susceptibility χ_{AF} , we obtain a transition to an AFM state as shown in the corresponding phase diagram in Fig (3)(b). Again a stronger Fermi-Bose coupling V tends to stabilise the d -wave state, in turn shifting the transition to the AFM state to higher values of U_{ff} . The transition to the AFM state appears at considerably higher U_{ff} than in⁶⁵, because the 2×2 cluster is known to strongly suppress antiferromagnetism^{68,72}, thus favoring the superconducting state.

From these observations it emerges that increasing V enhances both s - and d -wave (with s -wave being dominant for nearly-free fermions). Increasing U_{ff} increases the spin density wave fluctuations and suppresses s -wave pairing, as a result of which d -wave can become dominant over an extended regime in parameter space. This suggests that T_c for d -wave can be increased by increasing

both V and U_{ff} and staying near the line where s -wave becomes subdominant compared to d -wave. In the static mean-field study of Ref.³ the highest T_c for a NaK mixture was found at $\xi = 0.6$. For those parameters we find a maximal $T_c/t = 0.17$. Whereas Migdal-Eliashberg theories usually do not have a built-in mechanism that puts a limit on T_c , the gain stops here when U_{bf} is too large compared to U_{ff} and U_{bb} causing a mechanical instability towards phase-separation^{25,27}.

V. CONCLUSIONS

In this work we studied the antiferromagnetic and superconducting instabilities of Bose-Fermi-Mixtures in the limit where the bosons can be treated within the Bogoliubov approximation. We used a weak coupling Monte-Carlo cluster solver within the DCA-framework allowing us to distinguish between s - and d -wave pairing in the fermionic sector. The dominant pairing mechanism is determined by the relative sizes of the repulsive fermi-fermi interaction U_{ff} and the interactions induced by the bosons scaling with $V = U_{\text{bf}}^2/U_{\text{bb}}$ leading to the phase diagram shown in Fig (3)(a). In particular, we find that d -wave superconductivity can be stabilized by the presence of bosonic particles. This extends the results of a recent DMFT study⁶³ which found phases in which both bosons and fermions are superfluid, but could not determine the symmetry of the superfluid state. In addition, for strong Fermi-Fermi interaction, we observe a transition to an antiferromagnetic state suppressing the superconducting pairing as seen in Fig (3)(b), consistent with a previous study based on the functional renormalization group⁶⁵. Our approach holds whenever the bosonic speed of sound c is larger than the Fermi velocity v_{F} . We checked that for $c/v_{\text{F}} = 2$ the phase diagram looks similar but with stronger retardation effects. Our work can straightforwardly be extended to doped systems, allowing to address the strange metal physics and where also p -wave phases are predicted. The mechanisms discussed here are equally valid in 3d where T_c for d -wave could well be much higher than in $2d$.

Acknowledgments – We wish to thank M. Bukov and M. Punk for fruitful discussions and J. P. F. LeBlanc for providing testresults to benchmark our DCA code. This work is supported by EPSRC Grant EP/K030094/1 and FP7/ERC Starting Grant No. 306897. Use was made of the ALPS libraries^{80,81}. LP thanks the hospitality of the Aspen Center for Physics (NSF Grant No. 1066293).

Appendix A: Derivation of the effective action

In this appendix we explicitly discuss the construction of the effective action in Eq. 1. Starting from the Hamil-

tonian of Bose-Fermi-Mixtures on a 2D square lattice

$$\begin{aligned}
 H &= H_{\text{f}} + H_{\text{b}} + H_{\text{bf}} \\
 &= -t_{\text{f}} \sum_{\langle i,j \rangle, \sigma} c_{i,\sigma}^{\dagger} c_{j,\sigma} - \mu_{\text{f}} \sum_{i,\sigma} n_{i,\sigma}^{\text{f}} + U_{\text{ff}} \sum_i n_{i,\uparrow}^{\text{f}} n_{i,\downarrow}^{\text{f}} \\
 &\quad - t_{\text{b}} \sum_{\langle i,j \rangle} b_i^{\dagger} b_j - \mu_{\text{b}} \sum_i n_i^{\text{b}} + \frac{U_{\text{bb}}}{2} \sum_i n_i^{\text{b}} (n_i^{\text{b}} - 1) \\
 &\quad + U_{\text{bf}} \sum_{i,\sigma} n_i^{\text{b}} n_{i,\sigma}^{\text{f}}
 \end{aligned} \tag{A1}$$

where c_i^{\dagger} (b_i^{\dagger}) are fermionic (bosonic) creation operators at site i , $n_i^{f(b)}$ the corresponding densities, $t_{f(b)}$ describes the hopping of a fermion (boson) from site i to site j , $\mu_{f(b)}$ is the chemical potential for fermions (bosons), $U_{\text{ff}(bb)}$ is the on-site repulsion of fermions (bosons) and U_{bf} the on-site interaction between bosons and fermions. The model is the sum of a Fermi-Hubbard model (first line) the Bose-Hubbard model (second line) and a density-density interaction between bosons and fermions (third line). In the following we will treat the bosons within the Bogoliubov approximation allowing us to integrate them out in favour of a retarded density-density interaction between fermions.

In the Bogoliubov approximation the bosonic Hamiltonian H_{b} takes the form $H_{\text{b}} \approx \sum_{\mathbf{k}} E_{\mathbf{k}} a_{\mathbf{k}}^{\dagger} a_{\mathbf{k}}$ in terms of the Bogoliubov quasi-particles defined by $b_{\mathbf{k}} = u_{\mathbf{k}} a_{\mathbf{k}} - v_{\mathbf{k}} a_{-\mathbf{k}}^{\dagger}$ and $b_{\mathbf{k}}^{\dagger} = u_{\mathbf{k}} a_{\mathbf{k}}^{\dagger} - v_{\mathbf{k}} a_{-\mathbf{k}}$ respectively. As usual the coefficients are given by $u_{\mathbf{k}} = \cosh \phi_{\mathbf{k}}$ and $v_{\mathbf{k}} = \sinh \phi_{\mathbf{k}}$ where $\tanh 2\phi_{\mathbf{k}} = n_0 U_{\text{bb}} / (\bar{\epsilon}_{\mathbf{k}} + n_0 U_{\text{bb}})$. The Bogoliubov spectrum is given by $E_{\mathbf{k}} = [\bar{\epsilon}_{\mathbf{k}}^2 + 2\bar{\epsilon}_{\mathbf{k}} n_0 U_{\text{bb}}]^{1/2}$ with $\bar{\epsilon}_{\mathbf{k}} = \epsilon_{\mathbf{k}} - \epsilon_0$, the lattice dispersion of non-interacting bosons shifted to be positive. We emphasize that this treatment neglects any backaction of the fermionic sector on the bosons, in particular we assume that the bosons do not charge order, which limits our approach to the case of fast bosons.

Rewriting the coupling term H_{bf} in momentum space we obtain

$$H_{\text{bf}} = \frac{1}{N_s} \sum_{i, \vec{k}_1, \mathbf{k}_2} e^{-i(\mathbf{k}_1 - \mathbf{k}_2) \cdot \mathbf{r}_i} b_{\mathbf{k}_1}^{\dagger} b_{\mathbf{k}_2} n_i^{\text{f}} \tag{A2}$$

$$\begin{aligned}
 &= \frac{N_0}{N_s} \sum_i n_i^{\text{f}} + \frac{\sqrt{N_0}}{N_s} \sum'_{i, \mathbf{k}} \left(e^{i\mathbf{k} \cdot \mathbf{r}_i} b_{\mathbf{k}} + e^{-i\mathbf{k} \cdot \mathbf{r}_i} b_{\mathbf{k}}^{\dagger} \right) n_i^{\text{f}} \\
 &\quad + \frac{1}{N_s} \sum'_{i, \mathbf{k}_1, \mathbf{k}_2} e^{-i(\mathbf{k}_1 - \mathbf{k}_2) \cdot \mathbf{r}_i} b_{\mathbf{k}_1}^{\dagger} b_{\mathbf{k}_2} n_i^{\text{f}}
 \end{aligned} \tag{A3}$$

where N_0 is the macroscopic number of bosonic atoms in the condensate, N_s is the number of sites in the lattice and the primed sum indicates that the $k = 0$ terms should be omitted. In the following we will neglect the last term as it is suppressed by a power of $\sqrt{N_0}$ compared to the second term. The first term corresponds to the shift in the fermionic chemical potential present in

Eq. 1 whereas the second term represents the linear coupling of bosons to the fermions that will be integrated out.

Next, we reexpress the second term in the Bogoliubov boson operators to obtain

$$\begin{aligned} & \sum_{i\mathbf{k}}' \left(e^{i\mathbf{k}\mathbf{r}_i} b_{\mathbf{k}} + e^{-i\mathbf{k}\mathbf{r}_i} b_{\mathbf{k}}^\dagger \right) n_i^f \\ &= \sum_{i,\mathbf{k}}' \left(\alpha_{\mathbf{k}} [u_{\mathbf{k}} - v_{-\mathbf{k}}] e^{i\mathbf{k}\mathbf{r}_i} + \alpha_{\mathbf{k}}^\dagger [u_{\mathbf{k}} - v_{-\mathbf{k}}] e^{-i\mathbf{k}\mathbf{r}_i} \right) n_i^f. \end{aligned} \quad (\text{A4})$$

which clearly shows that the Bogoliubov bosons couple linearly to the fermionic density with momentum dependent couplings.

Employing coherent states for both the bosons and fermions the action reads as $S = S_f + S_{\text{bog}} + S_{\text{bf}}$ where the fermionic action S_f has already been defined in Eq. 1 and

$$S_{\text{bog}} = \int_0^\beta d\tau \sum_{\mathbf{k}} \bar{\alpha}_{\mathbf{k}}(\tau) \left[E_{\mathbf{k}} + \frac{\partial}{\partial \tau} \right] \alpha_{\mathbf{k}}(\tau) \quad (\text{A5})$$

$$\begin{aligned} S_{\text{bf}} &= \sqrt{n_0} U_{\text{bf}} \int_0^\beta d\tau \frac{1}{\sqrt{N_s}} \sum_{i,\mathbf{k}} \left(\alpha_{\mathbf{k}}(\tau) [u_{\mathbf{k}} - v_{-\mathbf{k}}] e^{i\mathbf{k}\mathbf{r}_i} \right. \\ &\quad \left. + \bar{\alpha}_{\mathbf{k}}(\tau) [u_{\mathbf{k}} - v_{-\mathbf{k}}] e^{-i\mathbf{k}\mathbf{r}_i} \right) n_i^f(\tau) \end{aligned} \quad (\text{A6})$$

Finally, integration over the quadratic bosonic Bogoliubov action yields the non-local, retarded density-density interaction, i.e. $e^{-S_{\text{ret}}} = \int d(\bar{\alpha}, \alpha) e^{-S_{\text{bog}} - S_{\text{bf}}}$ with

$$S_{\text{ret}} = -\frac{n_0 U_{\text{bf}}^2}{2} \iint_0^\beta d\tau_1 d\tau_2 \sum_{i,j} n_i^f(\tau_1) D_{ij}(\tau_1 - \tau_2) n_j^f(\tau_2) \quad (\text{A7})$$

which combined with S_f gives the total action $S = S_f + S_{\text{ret}}$ of the effective model in Eq. 1 and the kernel D_{ij} has been defined in Eq. 2.

Appendix B: Discussion of the sign problem

As we are at half-filling the simulations are sign-free for $V = 0$. However, as discussed in the main text the induced interactions lead to a sign-problem. The average sign of the simulations is shown in Fig. 6 in each panel at a fixed value of U_{ff} for different values of $V = U_{\text{bf}}^2/U_{\text{bb}}$.

We only observe a very weak dependence of the sign on the fermi-fermi interaction U_{ff} as expected from the sign free character for $V = 0$. In all cases the sign is exponentially decreasing as a function of β with a decay rate that increases as V is increased and the induced interactions become more important. This exponential dependence on the temperatures limits the lowest temperatures we can access in the simulations. Moreover,

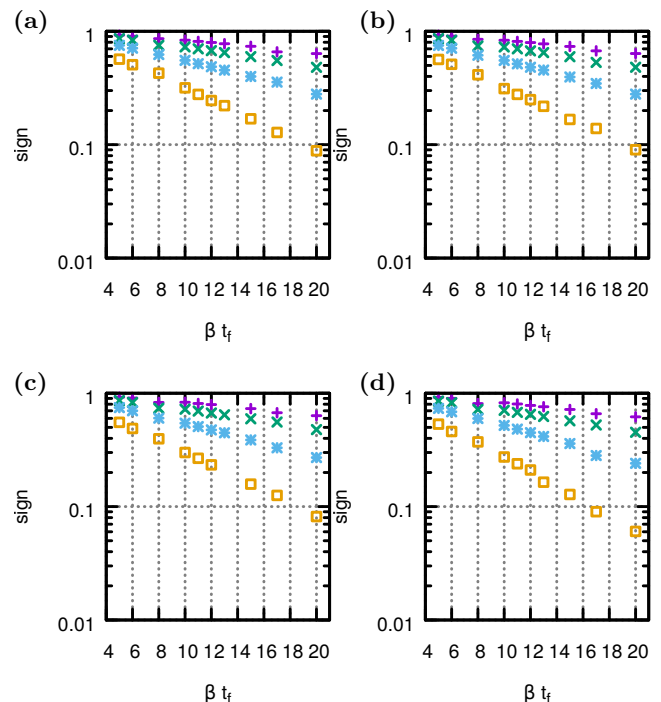


Figure 6. Average sign of the Monte-Carlo simulations as a function of β for $U_{\text{ff}}/t_f = 1, 2, 3, 4$ in panels (a)-(d), in each case for $V/t_f = 0.5, 1.0, 2.0, 4.0$ from top to bottom.

the strong dependence on the induced interactions limits the maximally accessible V and ultimately the extension to bigger clusters where the number of interaction terms proliferates.

* tb494@cam.ac.uk

¹ I. Bloch and W. Zwerger, Rev. Mod. Phys. **80**, 885–964 (2008).

² W. Ketterle and M. W. Zwierlein, Nuovo Cimento Rivista Serie **31**, 247 (2008), arXiv:0801.2500 [cond-mat.other].

³ D.-W. Wang, M. D. Lukin, and E. Demler, Phys. Rev.

A **72**, 051604 (2005).

⁴ D. J. Scalapino, E. Loh, and J. E. Hirsch, Phys. Rev. B **34**, 8190 (1986).

⁵ A. Abanov, A. V. Chubukov, and A. M. Finkel'stein, EPL (Europhysics Letters) **54**, 488 (2001).

⁶ A. Abanov, A. V. Chubukov, and J. Schmalian,

- Advances in Physics **52**, 119–218 (2003), <http://dx.doi.org/10.1080/0001873021000057123>.
- ⁷ Y. Wang and A. V. Chubukov, Phys. Rev. Lett. **110**, 127001 (2013).
 - ⁸ M. A. Metlitski and S. Sachdev, New Journal of Physics **12**, 105007 (2010).
 - ⁹ M. A. Metlitski and S. Sachdev, Phys. Rev. B **82**, 075128 (2010).
 - ¹⁰ E. Berg, M. A. Metlitski, and S. Sachdev, Science **338**, 1606 (2012), <http://www.sciencemag.org/content/338/6114/1606.full.pdf>.
 - ¹¹ E. G. Moon and S. Sachdev, Phys. Rev. B **80**, 035117 (2009).
 - ¹² S. Sachdev, M. A. Metlitski, and M. Punk, Journal of Physics: Condensed Matter **24**, 294205 (2012).
 - ¹³ D. J. Scalapino, Rev. Mod. Phys. **84**, 1383 (2012).
 - ¹⁴ H. Zhai, F. Wang, and D.-H. Lee, Phys. Rev. B **80**, 064517 (2009).
 - ¹⁵ E. G. Moon and S. Sachdev, Phys. Rev. B **82**, 104516 (2010).
 - ¹⁶ K. Kuroki, S. Onari, R. Arita, H. Usui, Y. Tanaka, H. Kontani, and H. Aoki, Phys. Rev. Lett. **101**, 087004 (2008).
 - ¹⁷ I. I. Mazin, D. J. Singh, M. D. Johannes, and M. H. Du, Phys. Rev. Lett. **101**, 057003 (2008).
 - ¹⁸ S. Graser, T. A. Maier, P. J. Hirschfeld, and D. J. Scalapino, New Journal of Physics **11**, 025016 (2009).
 - ¹⁹ S. Maiti and A. V. Chubukov, Phys. Rev. B **82**, 214515 (2010).
 - ²⁰ Paglione Johnpierre and Greene Richard L., Nat Phys **6**, 645–658 (2010), 10.1038/nphys1759.
 - ²¹ D. C. Johnston, Advances in Physics **59**, 803–1061 (2010), <http://dx.doi.org/10.1080/00018732.2010.513480>.
 - ²² Gegenwart Philipp, Si Qimiao, and Steglich Frank, Nat Phys **4**, 186–197 (2008), 10.1038/nphys892.
 - ²³ S. Nair, O. Stockert, U. Witte, M. Nicklas, R. Schedler, K. Kiefer, J. D. Thompson, A. D. Bianchi, Z. Fisk, S. Wirth, and F. Steglich, Proceedings of the National Academy of Sciences **107**, 9537 (2010), <http://www.pnas.org/content/107/21/9537.full.pdf>.
 - ²⁴ Z. Hadzibabic, C. A. Stan, K. Dieckmann, S. Gupta, M. W. Zwierlein, A. Görlitz, and W. Ketterle, Phys. Rev. Lett. **88**, 160401 (2002).
 - ²⁵ H. P. Büchler and G. Blatter, Phys. Rev. Lett. **91**, 130404 (2003).
 - ²⁶ M. Lewenstein, L. Santos, M. A. Baranov, and H. Fehrmann, Phys. Rev. Lett. **92**, 050401 (2004).
 - ²⁷ H. P. Büchler and G. Blatter, Phys. Rev. A **69**, 063603 (2004).
 - ²⁸ M. Cramer, J. Eisert, and F. Illuminati, Phys. Rev. Lett. **93**, 190405 (2004).
 - ²⁹ R. Roth and K. Burnett, Phys. Rev. A **69**, 021601 (2004).
 - ³⁰ C. Silber, S. Günther, C. Marzok, B. Deh, P. W. Courteille, and C. Zimmermann, Phys. Rev. Lett. **95**, 170408 (2005).
 - ³¹ C. Ospelkaus, S. Ospelkaus, L. Humbert, P. Ernst, K. Sengstock, and K. Bongs, Phys. Rev. Lett. **97**, 120402 (2006).
 - ³² S. Ospelkaus, C. Ospelkaus, L. Humbert, K. Sengstock, and K. Bongs, Phys. Rev. Lett. **97**, 120403 (2006).
 - ³³ K. Günter, T. Stöferle, H. Moritz, M. Köhl, and T. Esslinger, Physical Review Letters **96** (2006), 10.1103/physrevlett.96.180402.
 - ³⁴ S. Powell, S. Sachdev, and H. P. Büchler, Phys. Rev. B **72**, 024534 (2005).
 - ³⁵ K.-K. Ni, S. Ospelkaus, M. H. G. de Miranda, A. Pe'er, B. Neyenhuis, J. J. Zirbel, S. Kotochigova, P. S. Julienne, D. S. Jin, and J. Ye, Science **322**, 231 (2008), <http://www.sciencemag.org/content/322/5899/231.full.pdf>.
 - ³⁶ T. Best, S. Will, U. Schneider, L. Hackermüller, D. van Oosten, I. Bloch, and D.-S. Lühmann, Physical Review Letters **102** (2009), 10.1103/physrevlett.102.030408.
 - ³⁷ L. Pollet, M. Troyer, K. Van Houcke, and S. M. A. Rombouts, Phys. Rev. Lett. **96**, 190402 (2006).
 - ³⁸ L. Pollet, C. Kollath, U. Schollwöck, and M. Troyer, Phys. Rev. A **77**, 023608 (2008).
 - ³⁹ F. M. Marchetti, C. J. M. Mathy, D. A. Huse, and M. M. Parish, Phys. Rev. B **78**, 134517 (2008).
 - ⁴⁰ E. Fratini and P. Pieri, Phys. Rev. A **81**, 051605 (2010).
 - ⁴¹ A. H. Hansen, A. Khramov, W. H. Dowd, A. O. Jamison, V. V. Ivanov, and S. Gupta, Phys. Rev. A **84**, 011606 (2011).
 - ⁴² H. Hara, Y. Takasu, Y. Yamaoka, J. M. Doyle, and Y. Takahashi, Phys. Rev. Lett. **106**, 205304 (2011).
 - ⁴³ Z.-Q. Yu, S. Zhang, and H. Zhai, Phys. Rev. A **83**, 041603 (2011).
 - ⁴⁴ G. Bertaina, E. Fratini, S. Giorgini, and P. Pieri, Phys. Rev. Lett. **110**, 115303 (2013).
 - ⁴⁵ A. Guidini, G. Bertaina, D. E. Galli, and P. Pieri, Phys. Rev. A **91**, 023603 (2015).
 - ⁴⁶ I. Ferrier-Barbut, M. Delehaye, S. Laurent, A. T. Grier, M. Pierce, B. S. Rem, F. Chevy, and C. Salomon, Science **345**, 1035 (2014), <http://www.sciencemag.org/content/345/6200/1035.full.pdf>.
 - ⁴⁷ W. Zheng and H. Zhai, Phys. Rev. Lett. **113**, 265304 (2014).
 - ⁴⁸ J. J. Kinnunen and G. M. Bruun, Phys. Rev. A **91**, 041605 (2015).
 - ⁴⁹ C.-H. Wu, I. Santiago, J. W. Park, P. Ahmadi, and M. W. Zwierlein, Phys. Rev. A **84**, 011601 (2011).
 - ⁵⁰ J. W. Park, C.-H. Wu, I. Santiago, T. G. Tiecke, S. Will, P. Ahmadi, and M. W. Zwierlein, Phys. Rev. A **85** (2012), 10.1103/physreva.85.051602.
 - ⁵¹ J. W. Park, S. A. Will, and M. W. Zwierlein, Phys. Rev. Lett. **114**, 205302 (2015).
 - ⁵² M. Bijlsma, B. Heringa, and H. Stoof, Phys. Rev. A **61** (2000), 10.1103/physreva.61.053601.
 - ⁵³ H. Heiselberg, C. Pethick, H. Smith, and L. Viverit, Physical Review Letters **85**, 2418–2421 (2000).
 - ⁵⁴ G. Modugno, G. Roati, F. Riboli, F. Ferlaino, R. J. Brecha, and M. Inguscio, Science **297**, 2240 (2002), <http://www.sciencemag.org/content/297/5590/2240.full.pdf>.
 - ⁵⁵ L. Viverit, Phys. Rev. A **66**, 023605 (2002).
 - ⁵⁶ L. Viverit and S. Giorgini, Phys. Rev. A **66** (2002), 10.1103/physreva.66.063604.
 - ⁵⁷ F. Matera, Phys. Rev. A **68**, 043624 (2003).
 - ⁵⁸ M. Kagan, I. Brodsky, D. Efremov, and A. Klaptsov, Journal of Experimental and Theoretical Physics **99**, 640–646 (2004).
 - ⁵⁹ F. Illuminati and A. Albus, Phys. Rev. Lett. **93**, 090406 (2004).
 - ⁶⁰ D.-W. Wang, Phys. Rev. Lett. **96**, 140404 (2006).
 - ⁶¹ R. M. Kalas, A. V. Balatsky, and D. Mozyrsky, Phys. Rev. B **78**, 184513 (2008).
 - ⁶² T. Enss and W. Zwerger, The European Physical Journal B **68**, 383–389 (2009).
 - ⁶³ P. Anders, P. Werner, M. Troyer, M. Sgrist, and L. Pollet, Physical Review Letters **109** (2012), 10.1103/phys-

- revlett.109.206401.
- ⁶⁴ M. Bukov and L. Pollet, Phys. Rev. B **89** (2014), 10.1103/physrevb.89.094502.
- ⁶⁵ L. Mathey, S.-W. Tsai, and A. Neto, Physical Review Letters **97** (2006), 10.1103/physrevlett.97.030601.
- ⁶⁶ M. Hettler, A. Tahvildar-Zadeh, M. Jarrell, T. Pruschke, and H. Krishnamurthy, Phys. Rev. B **58**, R7475–R7479 (1998).
- ⁶⁷ M. Jarrell, T. Maier, C. Huscroft, and S. Moukouri, Phys. Rev. B **64** (2001), 10.1103/physrevb.64.195130.
- ⁶⁸ T. Maier, M. Jarrell, T. Pruschke, and M. Hettler, Rev. Mod. Phys. **77**, 1027–1080 (2005).
- ⁶⁹ A. N. Rubtsov and A. I. Lichtenstein, Journal of Experimental and Theoretical Physics Letters **80**, 61–65 (2004).
- ⁷⁰ A. Rubtsov, V. Savkin, and A. Lichtenstein, Phys. Rev. B **72** (2005), 10.1103/physrevb.72.035122.
- ⁷¹ F. Assaad and T. Lang, Phys. Rev. B **76** (2007), 10.1103/physrevb.76.035116.
- ⁷² T. Maier, M. Jarrell, T. Schulthess, P. Kent, and J. White, Physical Review Letters **95** (2005), 10.1103/physrevlett.95.237001.
- ⁷³ A. A. Abrikosov, *Methods of Quantum Field Theory in Statistical Physics (Dover Books on Physics)*, revised ed. (Dover Publications, 1975).
- ⁷⁴ A. B. Migdal, Sov. Phys. JETP **7**, 996 (1958).
- ⁷⁵ G. M. Eliashberg, Sov. Phys. JETP **11** (1960).
- ⁷⁶ J. P. Carbotte, Rev. Mod. Phys. **62**, 1027 (1990).
- ⁷⁷ F. Marsiglio and J. Carbotte, in *Superconductivity*, edited by K. Bennemann and J. Ketterson (Springer Berlin Heidelberg, 2008) p. 73–162.
- ⁷⁸ J. Bauer, J. E. Han, and O. Gunnarsson, Phys. Rev. B **84**, 184531 (2011).
- ⁷⁹ E. R. Margine and F. Giustino, Phys. Rev. B **87**, 024505 (2013).
- ⁸⁰ B. Bauer, L. D. Carr, H. G. Evertz, A. Feiguin, J. Freire, S. Fuchs, L. Gamper, J. Gukelberger, E. Gull, S. Guertler, A. Hehn, R. Igarashi, S. V. Isakov, D. Koop, P. N. Ma, P. Mates, H. Matsuo, O. Parcollet, G. Pawłowski, J. D. Picon, L. Pollet, E. Santos, V. W. Scarola, U. Schollwöck, C. Silva, B. Surer, S. Todo, S. Trebst, M. Troyer, M. L. Wall, P. Werner, and S. Wessel, Journal of Statistical Mechanics: Theory and Experiment **2011**, P05001 (2011).
- ⁸¹ E. Gull, P. Werner, S. Fuchs, B. Surer, T. Pruschke, and M. Troyer, Computer Physics Communications **182**, 1078 (2011).